North Dakota US12—Embankment Subgrade and Geogrid Stabilized Base Materials—August 2010

PROJECT DATE/DURATION
August 9 to 12, 2010

RESEARCH PROJECT TITLE
Accelerated Implementation of Intelligent Compaction Technology for Embankment Subgrade Soils, Aggregate Base, and Asphalt Pavement Materials (FHWA DTFH61-07-C-R0032)

SPONSOR
Federal Highway Administration

PRINCIPAL INVESTIGATOR
George Chang, Ph.D., P.E.
Project Manager
The Transtec Group, Inc.
512-451-6233

RESEARCH TEAM
David J. White, Ph.D.
Pavana KR. Vennapusa, Ph.D.
Heath Gieselman, M.S.
Jiake Zhang, M.S.
Michael Eidem

AUTHORS
David J. White, Ph.D.
Pavana KR. Vennapusa, Ph.D.
Department of Civil, Construction, and Environmental Engineering
Center for Earthworks Engineering Research

MORE INFORMATION
http://www.ceer.iastate.edu/research/project/project.cfm?projectID=-373342403

This document was developed as part of the Federal Highway Administration (FHWA) transportation pooled fund study TPF-5(233) – Technology Transfer for Intelligent Compaction Consortium (TTICC).

CENTER FOR CEER EARTHWORKS ENGINEERING RESEARCH
IOWA STATE UNIVERSITY
Institute for Transportation

Figure 1. Caterpillar CS56 smooth drum with padfoot shell kit (left) and Caterpillar CS563E smooth drum (right) rollers (from White et al. 2010)

INTRODUCTION

This demonstration was conducted on the US Highway 12 in Marmarth, North Dakota. The machine configurations and roller-integrated compaction measurement (RICM) systems used on this project included (Figure 1): a Caterpillar CP56 smooth drum roller with a padfoot shell kit (hereinafter referred to as padfoot roller) equipped with machine drive power (MDP), and a Caterpillar CS563E vibratory smooth drum roller equipped with MDP and compaction meter value (CMV) measurement technologies. (Note: MDP* values are reported as MDP*; see White et al. (2010) for description of MDP*). The machines were equipped with real time kinematic (RTK) global positioning system (GPS) and on-board display and documentation systems. The project involved construction and testing of seven test beds (TBs). Four of these TBs included silty subgrade materials and the remaining three included salvage base materials. The TBs with salvage base materials varied in terms of their underlying support conditions. One TB was reinforced with two layers of geogrid in the base layers, one TB was partially treated with over excavation and replacement due to soft subgrade conditions, and the other TB served as a control section with no special treatments.

The RICM values were evaluated by conducting field testing in conjunction with different point measurements: in situ dry density (γ_d) and moisture content (w) determined from nuclear gauge, California bearing ratio (CBR) determined from dynamic cone penetrometer (DCP) test, drained shear strength parameters from borehole shear test (BST), and dynamic modulus determined from falling weight deflectometer (FWD) and light weight deflectometer (LWD). The goals of this field study were to accomplish the following:

- Document machine vibration amplitude influence on compaction efficiency.
- Develop correlations between RICM values to traditional in-situ point measurements (point-MVs).
- Evaluate the impact of geogrid reinforcement in the base layers on RICM values and point-MVs in comparison with sections without reinforcement.
- Compare RICM results to traditional compaction operations.
- Study RICM values in production compaction operations.
- Evaluate RICM values in terms of alternative specification options.

MATERIALS

The silty subgrade material in the TBs was classified as silty sand (SM) and A-2-4 soil, and the salvage base material was classified as poorly graded sand with gravel (GM) and A-1-a.

SUMMARY OF KEY FINDINGS

Subgrade Test Beds Compacted with Padfoot Roller

Four subgrade test beds (TBs 1 to 3, and 7) were constructed and tested in this study. TB1 consisted of three side-by-side calibration lanes compacted in static, low amplitude (*a* = 0.90 mm), and high amplitude (*a* = 1.80 mm) modes. TB2 consisted of a one-dimensional test strip with visible rutting areas at the surface. TBs 3 and 7 consisted of production areas. Following are some key findings and conclusions from these TBs:

- MDP* data are influenced by the vibration amplitude settings used during compaction. Results from TB1 indicated that on average, MDP* generally increased with increasing number of passes when compacted in static and low amplitude mode, while in high amplitude mode the compaction growth curve yielded inconsistent results between passes (Figures 2 and 3). This is attributed to de-compaction of the material at the surface and possibly deeper compaction when high amplitude setting is used for compaction.

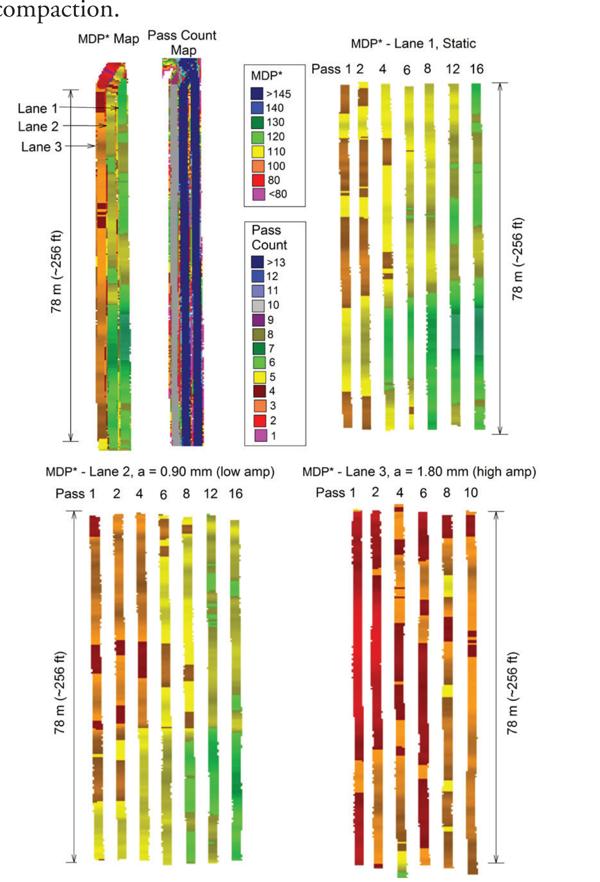

Figure 2. MDP and elevation maps of lanes 1 to 3, and MDP* spatial maps for multiple padfoot roller passes on lanes 1 to 3 – TB1 (from White et al. 2010)*

- The average MDP* values from TB1 obtained in low amplitude mode were either similar or slightly lower (by about 1.02 to 1.05 times) than the MDP* values obtained in static mode. The average MDP* values from TB3 production area in low amplitude mode were about 1.06 times lower than the MDP* values obtained in static mode.
- The average MDP* values from TB1 obtained in high amplitude mode were lower (by about 1.19 to 1.25 times) than the average MDP* values in static and low amplitude modes.
- The average LWD modulus and CBR were lower on low and high amplitude mode lanes, compared to the lanes compacted in static mode. In contrary, the average γ_d was greater on low and high amplitude mode lanes than on static mode lane (Figure 3).
- Regression analysis results between static MDP* and different point-MVs showed R^2 values ranging from 0.15 to 0.54. Static MDP* values were better correlated with LWD modulus (R^2 = 0.54) than with CBR (R^2 = 0.17) and γ_d (R^2 = 0.15) (Figure 4). This observation is generally consistent with findings from several previous case studies that the RICM values correlate better with stiffness or modulus measurements compared to density measurements. Correlations with low and high MDP generally showed weak relationships because of limited and narrow range of measurements.
- MDP* and LWD point-MVs obtained from TB2 effectively identified the soft/rutting areas observed at the surface (Figure 5).
- Geostatistical analysis on production area MDP* values indicated nested spherical variogram structures with short- and long-range spatial structures (Figure 6). The long-range spatial structures are

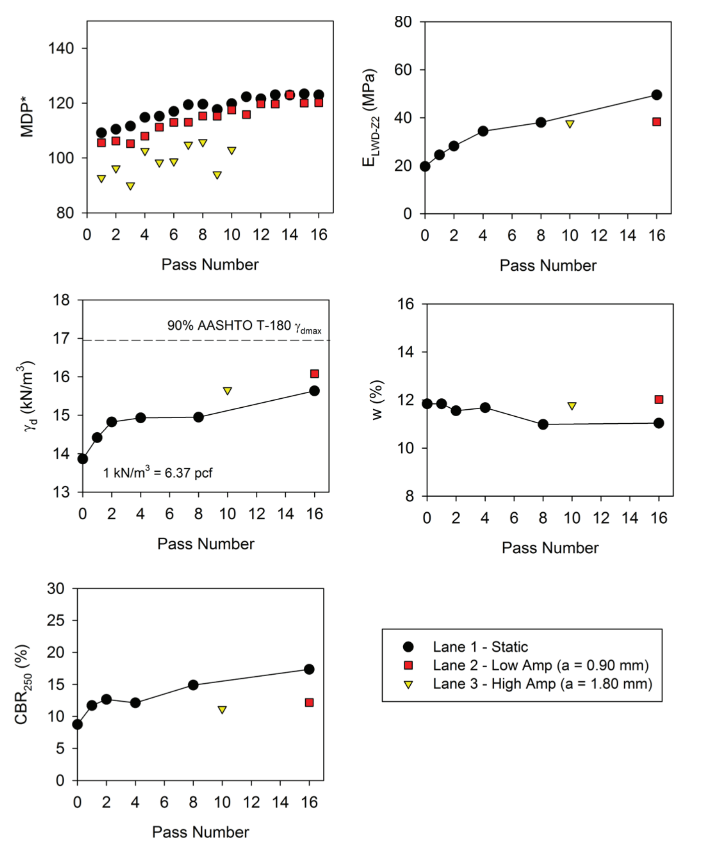

Figure 3. Average MDP and in-situ point measurement values with increasing roller passes on lanes 1 to 3 – TB1 (from White et al. 2010)*

likely linked to the spatial variation in the underlying support conditions while the short-range spatial structures are a result of soil properties close to the surface.

- The static MDP*values in TB3 production area showed more variability with high sill values compared to low amplitude MDP*. This was also evident with a slightly higher standard deviation (σ) value for static MDP* over low amplitude MDP* (Figure 6).

Salvage Base Materials (Control, Geogrid Reinforced, and Partial Core-out and Replace Sections) Compacted with Smooth Drum Roller

Three test beds were constructed and tested with salvage base material. TB4 consisted of two salvage base layers reinforced with two TX5 geogrid (Figure 7) layers, and were placed over compacted mixed subgrade+base. TB6 was partially treated with core-out and replacement with salvage base due to soft subgrade conditions. TB5 served as a control section with no treatments. On TB4, tests were conducted on the mixed subgrade+base layer, and the two salvage base layers. On TBs 5 and 6, tests were mostly conducted on the final surface of the salvage base layer. Following are the key findings from these test beds:

- CMV data showed relatively high variability (COV = 78 to 87%) compared to MDP* data (COV = 2%) on TB4 mixed subgrade+base layer. The LWD modulus and CBR point-MVs showed COV ranging between 30% and 64%. Variations observed in the points-MVs corroborated well with the variations in CMV while MDP* did not capture these variations.
- MDP* values were repeatable for forward passes but were affected by variable machine speed for reverse passes.

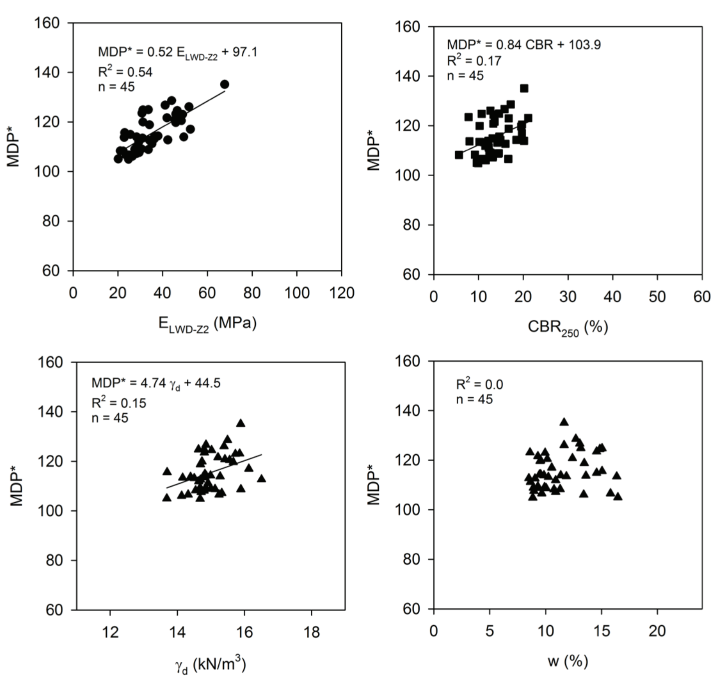

Figure 4. Correlations between MDP and in-situ point measurements on lane 1 (static) – TB1 (from White et al. 2010)*

- Results on TB4 indicate that the MDP* and the point-MVs are relatively high and less variable on salvage base layer 1 than on the underlying mixed subgrade layer. On salvage base layer 2, the point-MVs are on average higher on base layer 2 than on the underlying base layer 1 and the mixed subgrade layer. The average MDP* and COV of MDP* were about the same on base layers 1 and 2.
- Variations observed in DCP-CBR profiles corroborated well with variations observed in the BST effective shear strength measurements (i.e., cohesion *c*' and effective angle of internal friction ϕ') with depth in the base and subgrade layers.
- The average MDP* from TB6 control section (i.e., outside the core-out area) was lower (by about 1.06 times) and the COV of MDP* was greater than on TB4 (1% on TB4 and 4% on TB6) (Figure 8). The LWD and FWD modulus values in the control section were also on average lower (by about 1.1 to 1.6 times) than on TB4. However, it must be noted that only a limited number of point-MVs (1 to 4) were obtained in this area.
- MDP* values were slightly lower (by about 1.04 times) on TB5 control section than on the TB4 geogrid reinforced section. The FWD modulus values were also on average slightly lower (by about 1.1 times) on TB5 than on TB4, while the average the LWD modulus values were about the same. The COV of MDP* and point-MVs on TBs 4 and 5 were quite similar.

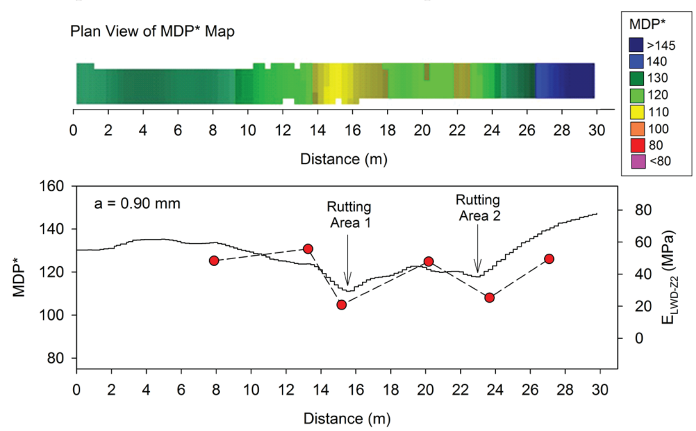

Figure 5. MDP and LWD measurements on TB2 (from White et al. 2010)*

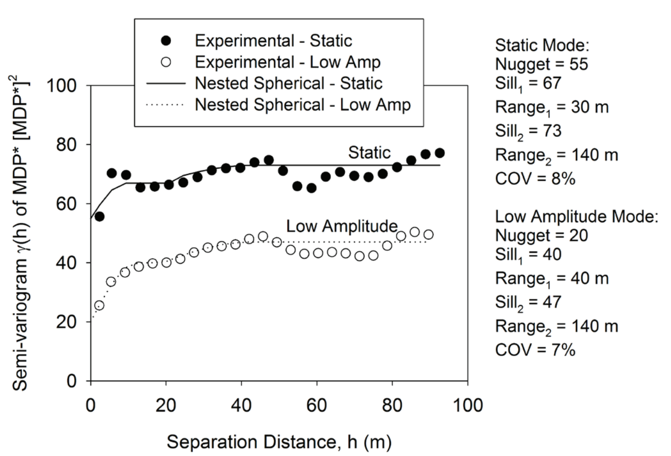

Figure 6. Histograms and geostatistical semivariograms of MDP from static and low amplitude mapping passes – TB3 production area*

- Although the relationships generally showed correct trends, they were weak ($R^2 < 0.5$) for all MDP* correlations with point-MVs (Figure 9). The primary reason for such weak correlations is attributed to the narrow MDP* measurement range (varied between 135 and 149). Also, different trends were observed for TB4 and TB5 for MDP* vs. E_{LWD-Z3} and MDP* vs. E_{FWD-K3} relationships. This is likely because of differences in underlying support conditions. No information was available from TB5 to assess those conditions.

Figure 7. TX5 geogrid used in TB4 (from White et al. 2010)

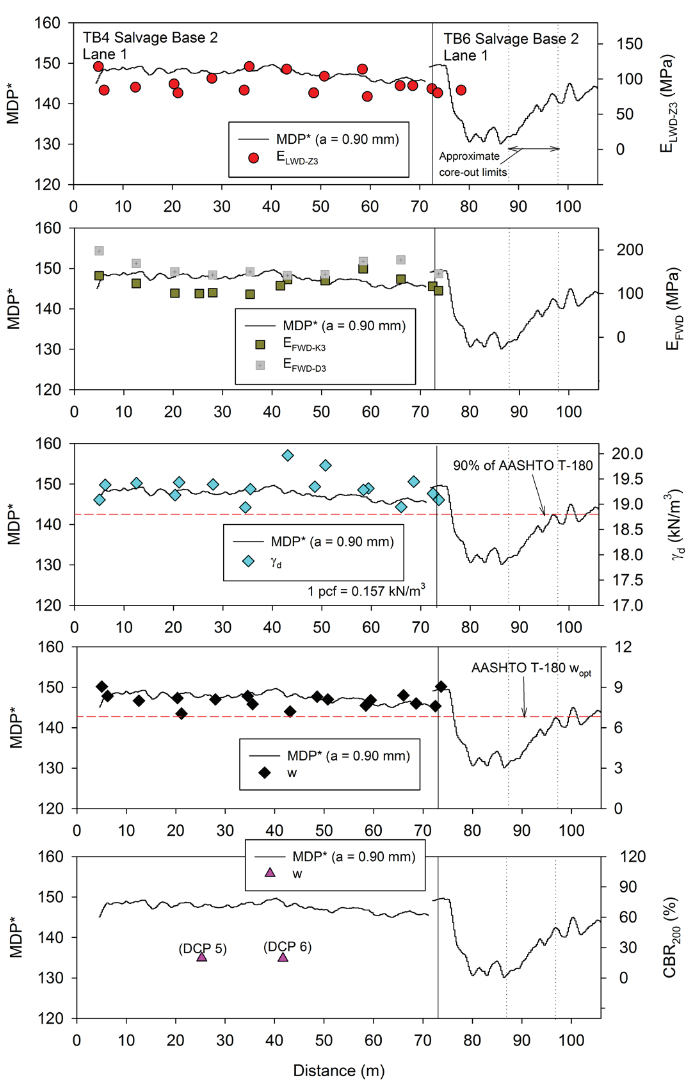

Figure 8. Comparison of MDP measurements and in-situ point measurements on salvage base layer 2 lane 1 – TBs 4 and 6*

- CMV correlations with E_{FWD-K3} and CBR yielded $R^2 > 0.5$, while correlations with E_{LWD-Z3} yielded $R^2 = 0.35$ (Figure 10). No statistically significant relationship was observed between CMV and E_{FWD-D3}.

REFERENCES

White, D.J., Vennapusa, P., Gieselman, H., Johanson, L., Goldsmith, R. (2010). Accelerated Implementation of Intelligent Compaction Monitoring Technology for Embankment Subgrade Soils, Aggregate Base, and Asphalt Pavement Materials TPF-5(128) – US12 Marmarth, North Dakotat, Report submitted to The Transtec Group, FHWA, November.

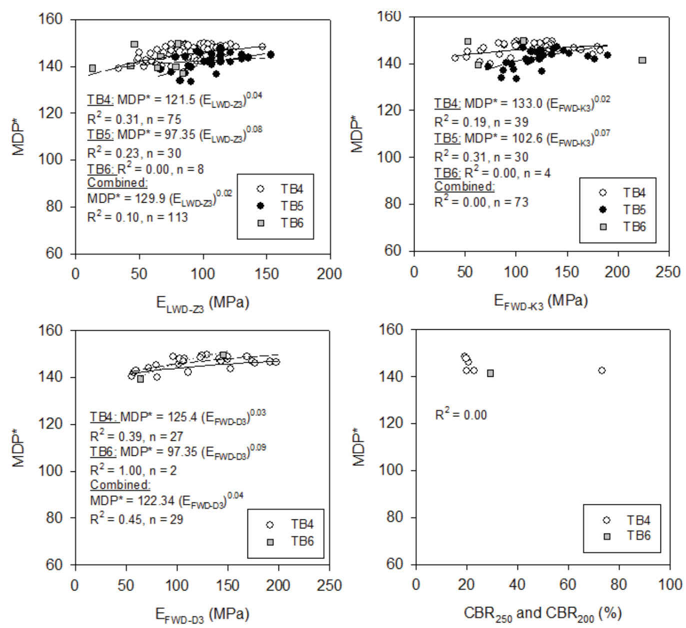

Figure 9. Correlations between MDP (a = 0.90 mm and f = 30 Hz) and point-MVs - TBs 4, 5, and 6 (from White et al. 2010)*

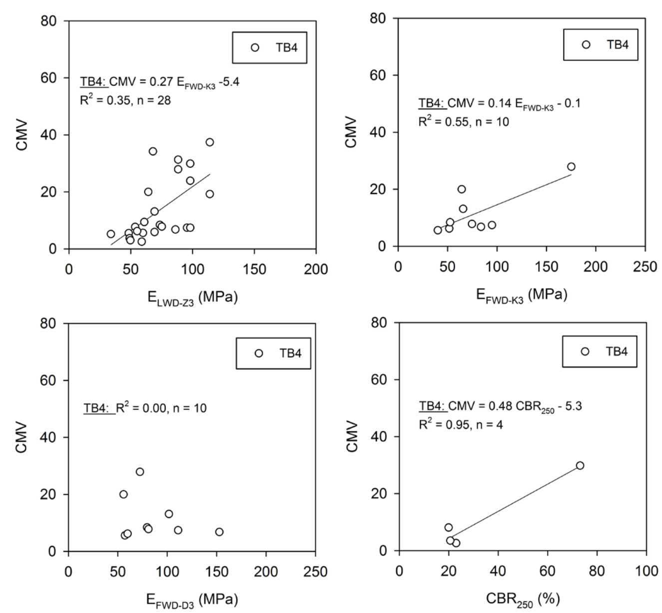

Figure 10. Correlations between CMV (a = 0.90 mm and f = 30 Hz) and point-MVs - TB 4 (from White et al. 2010)